

Diffractive Measurements in ATLAS

K. Shaw (on behalf of the ATLAS collaboration)

INFN Gruppo Collegato di Udine and ICTP, Italy

Abstract. Measurements made using the ATLAS detector at the LHC at $\sqrt{s} = 7$ TeV incorporating diffractive processes are presented. A first measurement of the inelastic cross-section using $20 \mu\text{b}^{-1}$ of data is given, yielding a result of $\sigma_{inel}(\xi > 5 \times 10^{-6}) = 60.3 \pm 2.1$ mb, for single ($pp \rightarrow Xp$) and double ($pp \rightarrow XY$) diffractive processes for a kinematic range corresponding to detector acceptance $\xi = M_X^2/s$ calculated from the invariant mass M_X of the heavier dissociation system X. Furthermore a study is made of pseudorapidity gap distributions using $7.1 \pm 0.2 \mu\text{b}^{-1}$ of data collected to tune the diffractive fraction of the inelastic cross-section in Monte Carlo (MC) models, and a measurement is made of the differential cross-section for events with large gaps in pseudorapidity where diffractive processes dominate.

PACS: 13.85.-t

INTRODUCTION

Diffractive processes are of interest to study as they are the dominant contribution to high-energy elastic and quasi-elastic scattering in hadron interactions and they contribute to the total cross-section which cannot be calculated directly from Quantum Chromodynamics (QCD). Moreover in the high particle multiplicity environment of the Large Hadron Collider (LHC), it is of great importance to describe the large number of additional pp interactions in each bunch crossing, which has a significant contribution from diffractive dissociation. Thus using the ATLAS detector [1] at the LHC a first measurement has been made of the inelastic cross-section [2] and a study of pseudorapidity gap¹ signatures of diffractive events [3] has been performed resulting in a first measurement of the differential cross-section.

The total pp cross-section at the LHC can be divided into elastic (el) and inelastic (inel) components. The inelastic part is further divided into single diffractive (sd), double diffractive (dd), central diffractive (cd) and non-diffractive (nd) components, $\sigma_{tot} = \sigma_{el} + \sigma_{sd} + \sigma_{dd} + \sigma_{cd} + \sigma_{nd}$. Only non-diffractive inelastic events involve a colour exchange between the colliding partons. In diffractive events there is a colour singlet exchange, which can be described using Regge theory [5] as a Pomeron, resulting in large gaps in pseudorapidity² (η) between the proton dissociation products, where the debris is produced in the very forward regions of the detector.

For these measurements Minimum Bias Trigger Scintillators (MBTS) were used to trigger on activity on only one side (single-sided) or both sides (inclusive) of the interaction point (IP), and consist of two sets of sixteen scintillator counters situated on the inner face of the endcap tile calorimeter in the forward regions of ATLAS. Additionally the ATLAS inner detector and calorimeters provide information on particle activity distributions in pseudorapidity.

MEASUREMENT OF THE INELASTIC CROSS-SECTION

Using an integrated luminosity of $20.3 \pm 0.7 \mu\text{b}^{-1}$ at $\sqrt{s} = 7$ TeV in 2010 the inelastic pp cross-section has been measured using an inclusive event sample selecting events where at least two MBTS scintillating counters detect a charge larger than some threshold, known as hits. Additionally to constrain the diffractive component of the inclusive sample, single-sided events were selected where one side of the MBTS detector contained at least two hits, and the other side detected no hits.

The measurement is limited to events where the dissociation systems have a large invariant mass (M_X , where X denotes the larger (only) dissociative mass system separated by a rapidity gap with the other dissociative mass system (proton) in double (single) diffractive events), as these are outside the acceptance of the MBTS corresponding to $\xi =$

¹ Known as simply ‘rapidity gaps’ for the remainder of the note.

² Pseudorapidity is defined in terms of the polar angle θ as $\eta = -\ln \tan(\theta/2)$.

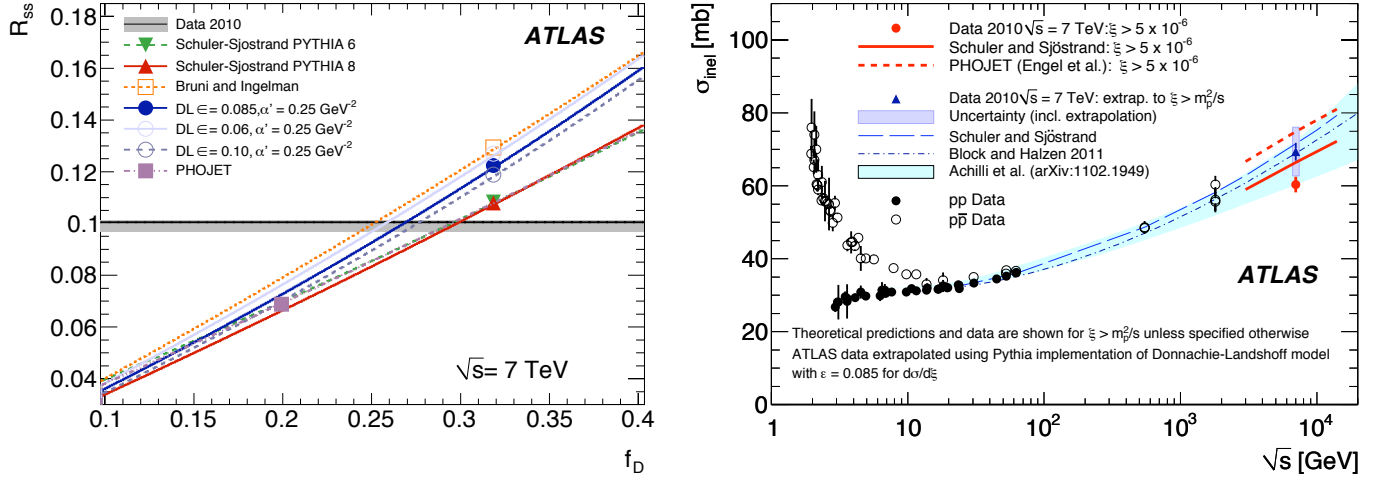


FIGURE 1. The left-hand plot shows the uncorrected ratio R_{ss} of single-sided events, dominated by diffractive processes, to inclusive events, dominated by non-diffractive processes, as a function of the fractional contribution of diffractive events to the inclusive sample (f_D). The right-hand plot shows the inelastic cross-section as a function of \sqrt{s} where the ATLAS measurement for $\xi > 5 \times 10^{-6}$ is shown (red filled circle) and the measurement extrapolated to the full inelastic cross-section is shown (blue triangle) with error bars indicating the associated uncertainty including the extrapolation uncertainty (blue shaded area).

$M_X^2/s > 5 \times 10^{-6}$, equivalent to $M_X > 15.7$ GeV. Thus the inelastic cross-section has been measured according to Equation 1, where $N(N_{BG})$ denotes the number of selected (background) events within the MBTS acceptance, $\int L dt$ is the integrated luminosity, $\epsilon_{trig}(\epsilon_{sel})$ is the trigger (selection) efficiency in the ξ -range and $f_{\xi < 5 \times 10^{-6}}$ is the fraction of events that pass the event selection with $\xi < 5 \times 10^{-6}$.

$$\sigma(\xi > 5 \times 10^{-6}) = \frac{N - N_{BG}}{\epsilon_{trig} \times \int L dt} \frac{1 - f_{\xi < 5 \times 10^{-6}}}{\epsilon_{sel}} \quad (1)$$

The fractional contribution of diffractive events ($f_D = \sigma_{sd} + \sigma_{dd} / \sigma_{inel}$) to the total inelastic cross-section varies significantly between models. Thus the ratio of single-sided to inclusive events (R_{ss}) in data, measured to be $R_{ss,(data)} = 10.02 \pm 0.03(\text{stat.}) \pm 0.1(\text{syst.})\%$, is sensitive to f_D in the MC models and therefore can be used to constrain f_D . The left-hand plot in Figure 1 compares $R_{ss,(data)}$ to R_{ss} predicted from a variety of MC generators with varying values of f_D , where their intersection with the $R_{ss,(data)}$ is used as the central value for f_D for that model. Using the default DL model [4] the resulting value is $f_D = 26.9^{2.5}_{-1.0}\%$ and this tuned model is used to calculate MC dependent corrections to the cross-section measurement.

The inelastic cross-section has been measured as $\sigma_{inel}(\xi > 5 \times 10^{-6}) = 60.3 \pm 0.05(\text{stat.}) \pm 0.5(\text{syst.}) \pm 2.1$ (lumi) mb. Furthermore to compare this with previous results the measurement has been extrapolated to the full inelastic cross-section giving $\sigma_{inel}(\xi > m_p^2/s) = 69.4 \pm 2.4$ (exp.) ± 6.9 (extr.) mb and is shown on the right-hand plot in Figure 1 with the kinematically constrained measurement and compared with several MC predictions.

DIFFERENTIAL CROSS-SECTION MEASUREMENTS FOR RAPIDITY GAPS

The diffractive contribution to the inelastic cross-section has been tuned using $7.1 \pm 0.2 \mu\text{b}^{-1}$ of data and the differential cross-section has been measured. The measurement of the masses of dissociative system(s) is complicated by the fact that much of the debris is produced beyond the acceptance of the detector. A method has been developed to obtain the cross-section as a function of the size of the visible part of the rapidity gap separating the two systems (X and Y) in the case of double-diffractive processes, or separating the dissociative system from the elastically scattered proton in the case of single-diffractive processes. Rapidity gaps are identified by dividing the ATLAS calorimeters and inner detector into rings in η and identifying the largest sequential runs of rings without any particle activity in them, known as empty rings, starting from the edge of the acceptance ($\eta = \pm 4.9$) and of size $(\Delta\eta^F)$. Particle activity is

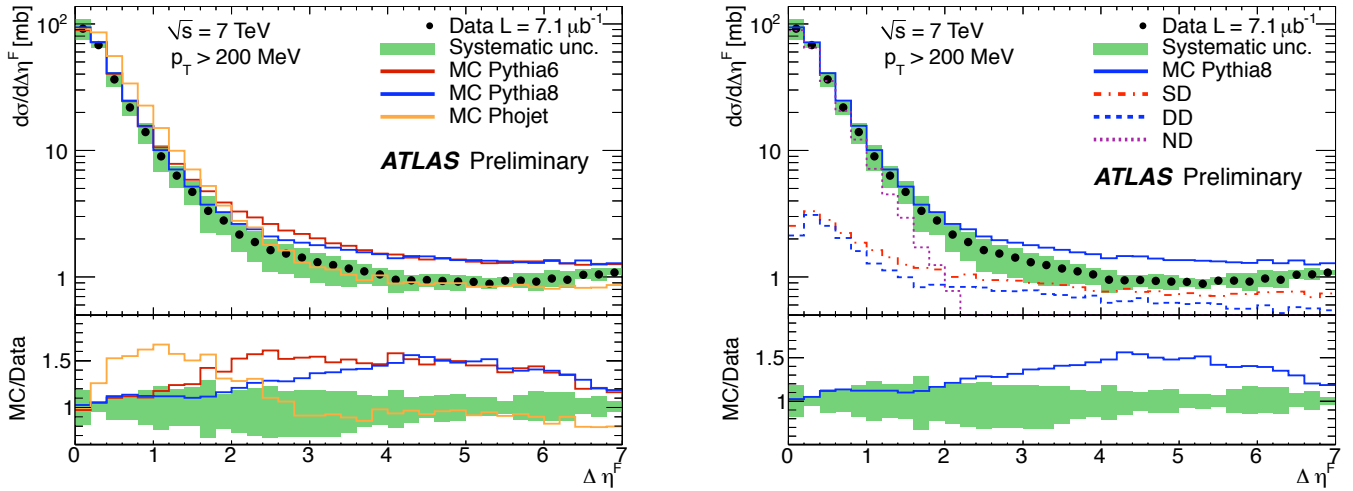


FIGURE 2. Inelastic cross-section shown as a function of rapidity gap size ($\Delta\eta^F$) for particles with $p_T > 200$ MeV corrected for experimental effects. Left-hand plot shows a comparison between various MC models and data and the right-hand plot shows the cross-section for only the default Pythia8 MC generator, with the single, double and non-diffractive contributions shown separately.

defined in the calorimeter as a cell above a chosen threshold, and in the tracker as a reconstructed track where the $p_T > 200$ MeV, $|\eta| < 2.5$. MC generators such as Pythia [6] and Phojet [7] have varying values of f_D . Thus these fractions were optimised for each model by fitting their diffractive and non-diffractive components to detector level data. This optimized fraction was found for the default MC generator Pythia8 to be $f_D = 30.2 \pm 0.3(\text{stat.}) \pm 3.8(\text{syst.})\%$.

The left-hand plot of Figure 2 shows the measured differential inelastic cross-section ($d\sigma/d\Delta\eta^F$) compared to various MC generators which shows at small (large) $\Delta\eta^F$ the Pythia (Phojet) MC describes the data best. The right-hand plot presents the different contributions to the cross-section for Pythia 8 MC generator showing at small (large) values of $\Delta\eta^F$ the non-diffractive (diffractive) component dominates. The diffractive cross-section has been measured as $d\sigma/d\Delta\eta^F \approx 1.0 \pm 0.2$ mb per unit of $\Delta\eta^F$ at high $\Delta\eta^F$ for $p_T > 200$ MeV.

CONCLUSION

A first measurement of the inelastic cross-section at $\sqrt{s} = 7$ TeV has been presented limited to the kinematic range corresponding to the acceptance of the ATLAS detector $\xi > 5 \times 10^{-6}$. Additionally the inelastic cross-section has been measured as a function of forward rapidity gaps.

REFERENCES

1. ATLAS Collaboration, "The ATLAS Experiment at the CERN Large Hadron Collider", *JINST* **3** (2008).
2. ATLAS Collaboration, "Measurement of the Inelastic Proton-Proton Cross-Section at $\sqrt{s} = 7$ TeV with the ATLAS Detector", *Nat Commun.*, **2**, 463 (2011).
3. ATLAS Collaboration, "Rapidity Gap Cross Sections in pp Interactions at $\sqrt{s} = 7$ TeV", ATLAS-CONF-2011-059 (2011).
4. A. Donnachie and P. V. Landshoff, "Elastic scattering and diffraction dissociation", *Nucl. Phys. B* **244**, 322-336 (1984).
5. T. Regge, "Introduction to complex orbital momenta", *Nuovo Cim.* **14**, 951 (1959).
6. T. Sjostrand, S. Mrenna and P. Skands, "PYTHIA 6.4 Physics and Manual", *JHEP* **05**, 026 (2006).
7. R. Engel, "Photoproduction within the two component dual parton model. 1. Amplitude and cross-sections", *Z. Phys* **C66**, 023 (1995).